

SPECTRAL CHANGES INDUCED BY THE ZEEMAN EFFECT IN OBLIQUE ROTATOR MODELS

ERMANN F. BORRA

Hale Observatories, Carnegie Institution of Washington, California Institute of Technology

Received 1973 November 26; revised 1974 June 12

ABSTRACT

Computations of line profiles for oblique rotator models show spectral variations induced by the Zeeman effect. It is found that the Zeeman effect and rotational Doppler shifts can cause asymmetries in the line profiles. The asymmetries can result in radial velocity variations. It is suggested that this effect could be used to search for magnetic fields in conditions where other methods fail. The magnetic star HD 10783 is interpreted as an example of the effect proposed. The Zeeman effect can also cause apparent changes in equivalent width.

Subject headings: line profiles — magnetic stars — Zeeman effect

I. INTRODUCTION

It is well known that the magnetic fields of the Ap stars affect the appearance of the spectral lines. Babcock (1949) has discussed the intensification of the equivalent width of saturated spectral lines formed in a magnetic field. Preston (1971) has found examples of stars in which the widths of the Zeeman broadened lines change throughout the magnetic cycle because of the changing value of the surface field.

In this work, we will consider other subtle effects of the magnetic field which, to the best of my knowledge, have never been considered in the astronomical literature.

II. ASYMMETRIES IN LINE PROFILES AND RADIAL VELOCITY VARIATIONS

Theoretical models for the Zeeman-analyzed line profiles in oblique rotator models have been discussed by Borra (1974*a*, Paper I) and Borra (1974*b*, Paper II). The surface of the star, after imposing a configuration of the magnetic field geometry, is subdivided in slices of about equal surface area. The Stokes parameters are computed for each slice using Unno's (1956) analytic solutions to the equations of transfer for a spectral line formed in the presence of a magnetic field, under the LTE Milne-Eddington approximation. Rotation is taken into account, and the Stokes parameters are integrated over the visible disk of the star. The first Stokes parameter gives the line profile. The geometry of the magnetic field is taken to be of the decentered dipole type (Landstreet 1970; see this reference and Papers I and II for details and parameters of the model).

Examination of the line profiles of the models of Papers I and II and of several other unpublished models reveal asymmetries in the profiles during part of the magnetic cycle. This is surprising because the abundance of the ion considered is taken to be constant over the surface of the star. The asymmetries can be quite conspicuous for models with large magnetic fields. However, even when the asymmetries are less noticeable, they will result in measurable radial velocity

variations if a portion of the line is emphasized when measuring radial velocities in photographic plates. In the following we will consider emphasizing of the core of the lines.

The radial velocities resulting from asymmetries have been computed from the line profiles. First, the theoretical profiles are convolved with a Gaussian instrumental profile of 0.07 Å half-width. A photographic characteristic curve is then applied for an optimum photographic exposure. We thus obtain a transmission profile that is then normalized to 0.0 at the continuum and 1.0 at maximum transmission. We obtain values for the radial velocities from the usual Doppler formula $\Delta\lambda/\lambda = v/c$ with $\Delta\lambda = \lambda_e - \lambda_0$, where λ_0 is the rest wavelength and λ_e is computed from

$$\lambda_e = \frac{\int r(\lambda)\lambda d\lambda}{\int r(\lambda)d\lambda}, \quad (1)$$

where $r(\lambda)$ represents the normalized transmission profile. The wavelength is 4260 Å, and the g -value for the simple triplet-splitting assumed is taken to be 1.2.

Only the part of the transmission profiles greater than 0.7 (30 percent from the point of highest transmission) is used in computing λ_e from equation (1) to obtain v_3 ; only the part greater than 0.3 (70 percent from the point of highest transmission) to obtain v_7 . The quantities v_3 and v_7 are useful in indicating the changes in the radial velocities when different parts of the lines are emphasized during the reductions. In figure 1 we have plotted, for half the cycle, the quantities v_3 and v_7 for three of the decentered dipole models described in Paper II. The rotational velocity is 15 km s⁻¹, the axis of rotation is at 90° with respect to the line of sight, the axis of symmetry of the dipole is perpendicular to the rotational axis, and the surface field at the strongest pole on the surface of the star is 10,000 gauss. The curves are identified with the parameter a , which measures the displacement of the dipole from the center of the star, in units of the stellar radius. In figure 2, we have v_3 and v_7 for one of the models of Paper I. The dipole axis is at 90° to the

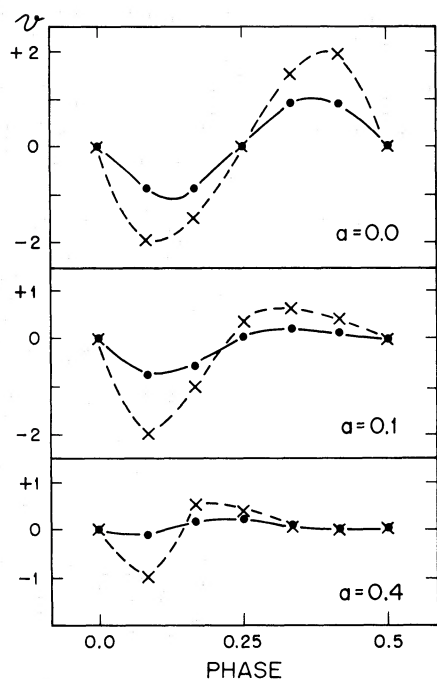


FIG. 1.—The quantities v_7 (full line) and v_3 (broken line) are expressed in km s^{-1} and plotted during half the cycle for the models with a magnetic field of 10,000 gauss at the strongest pole. The graphs are identified with the value of the decentering parameter a .

rotation axis, which is inclined at 30° with respect to the light of sight. The decentering parameter a is set at 0.3, the polar field is 30,000 gauss, and the equatorial velocity is 20 km s^{-1} . Phase 0.0 of the models is taken to be when the line of sight lies in the plane defined by the axis of rotation and dipole axis, the observer viewing the strongest pole on the surface of the star. This corresponds to one of the extrema of the longitudinal field variations, the other occurring at phase 0.5.

To understand the spectral variations we must consider the geometry of the magnetic field. Let us examine the centered dipole model of figure 1 ($a = 0.0$). At the poles, the magnetic field of 10,000 gauss will separate the σ components by 0.204 \AA (for a wavelength of 4260 \AA and a g -value = 1.2); thus we have a spectral feature broader and more shallow than in the zero-field case. At the equator, the field strength has decreased by a factor of 2; thus the σ components will be separated by 0.102 \AA and we have a spectral feature sharper and deeper than at the pole. It is the relative Doppler shifts between these features of differing width and depth which causes the asymmetries in the line profiles. Things are further complicated because the relative strength of the π and σ components changes with the inclination of the lines of force on the line of sight, thus changing the shape of the spectral line resulting for each slice.

The amplitude and shape of the radial velocity curves depend on the magnetic geometry, strength of the magnetic field (or z -value of the line considered), and

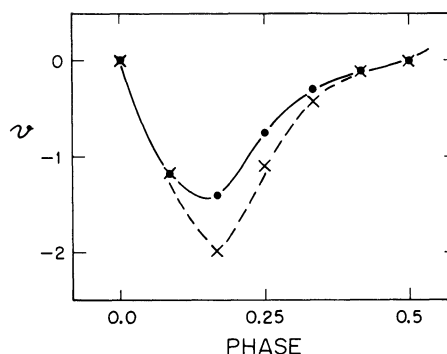


FIG. 2.—The quantities v_7 (full line) and v_3 (broken line) are expressed in km s^{-1} and plotted during half the cycle for the model with a magnetic field of 30,000 gauss at the strongest pole and 20 km s^{-1} equatorial velocity.

$v \sin i$. Figure 1 shows changes in the curves when the decentering parameter a is changed (keeping the polar field constant). For obvious reasons, the amplitude of the radial velocity curve will always be smaller than $v \sin i$. The amplitude also tends to increase with increasing surface field. A model similar to the $a = 4$ model of figure 1, but with a polar field of 30,000 gauss, had an amplitude almost 10 times larger between phase 0.0 and 0.25.

Preston and Stępień (1968) report a small-amplitude radial velocity variation, with the same period of the light and magnetic variations, in HD 10783. The star does not exhibit noticeable spectrum variations. Preston and Stępień propose an interpretation of the radial velocity variations based on greater contribution to the line profile from a region of higher than average surface brightness. However, it is questionable whether this explanation will survive a quantitative test (I am grateful to Dr. G. W. Preston for expressing to me his doubts on his earlier interpretation).

In a first order expansion, a displacement $\delta\lambda$ of a symmetrical spectral line results, for a fixed wavelength, in a flux change $\Delta F \propto F^{-1}(dF/d\lambda)\delta\lambda$, where $dF/d\lambda$ is the slope of the wing of the line and the monochromatic flux F is expressed in units of the continuum flux. In Preston and Stępień's interpretation, this change in flux is caused by the Doppler-shifted contribution to the line profile from the bright spot. If we take as a reasonable value $dF/d\lambda \sim 1.0$ and take $\delta\lambda = 0.015 \text{ \AA}$ (1 km s^{-1} at 4500 \AA), we see that we need a flux change ~ 1.5 percent caused by the bright spot. If we inspect the light curve of HD 10783 (Preston and Stępień 1968), we see that the maximum amplitude of the B light curve is about 4 percent. It is also apparent that the light curve is far from being sinusoidal, as we would expect if the bright spot occupied a significant portion of the stellar surface seen by the observer. The light curve is rather characterized by a bump lasting about a third of the cycle. To reproduce this type of light curve we need a relatively small bright region that is occulted for two-thirds of the cycle. At phases 0.25 and 0.75, where the maximum amplitude of the radial velocity curve occurs, the light curve does not deviate appreciably from its value at phase 0.5.

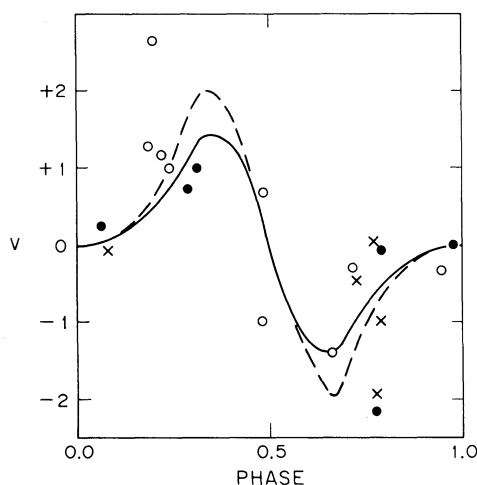


FIG. 3.—The theoretical radial velocity curves v_7 (full line) and v_3 (broken line) for the model of fig. 2 are plotted (after changing the theoretical phase convention) with the observed radial velocity observations for HD 10783. The star's γ -velocity ($\sim 20 \text{ km s}^{-1}$) has been subtracted from the observations which are plotted with the symbols used by Preston and Stepień (1968).

Therefore, we must conclude that at these phases the spot is not seen and does not contribute to the line profiles. An additional problem with a small spot is that it has to be hotter than the rest of the star. If the spot is made small enough, the temperature difference is such as to change significantly the equivalent widths of the lines formed in the spot. The radial velocity changes in such a situation are not simple, as the sign of the radial velocity will be different according to whether the equivalent width of a line is decreased or increased in the spot.

Let us now try to understand the radial velocity variations of HD 10783 in terms of the Zeeman effect, and let us attempt to draw inferences regarding the geometry of the magnetic field. The matching of a theoretical radial velocity curve with the observations depends on the parameters chosen for the decentered dipole model and depends critically on the phase of HD 10783 at which the surface field is at maximum. If we take the model figure 2 as an approximation for HD 10783, we obtain a plausible fit to the radial velocity curve of HD 10783, provided phase 0.0 of the model (H_s is at maximum) is identified with phase 0.5 of figure 1 of Preston and Stepień (1968). In figure 3 we have plotted v_3 and v_7 (after changing the theoretical phase convention) with the observed radial velocities in Preston and Stepień (1968). The signs, amplitude, and shape are reproduced within the observational errors. In any event, we would not expect the fit to be perfect, as the parameters of the model are probably only a rough approximation to HD 10783 and v_3 and v_7 probably do not reproduce exactly the weight that the eye gives to different parts of the line profiles.

The critical part of the fit between theory and observations depends on the identification of the phase

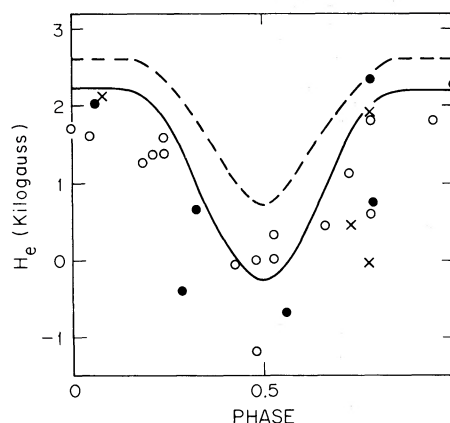


FIG. 4.—The theoretical longitudinal magnetic field curve H_{e7} (full line) and H_{e3} (broken line) for the model of fig. 2 are plotted (after changing sign and theoretical phase convention) with the observed longitudinal field of HD 10783. The symbols used for the observed magnetic fields are as in Preston and Stepień (1968). See text for more details.

of the magnetic cycle of HD 10783 at which the surface field H_s is at maximum (phase 0.0 of the theoretical model). Let us follow the arguments which originally prompted the writer to take the model of figure 2 as a reasonable approximation for HD 10783. In Papers I and II it is argued that, if the cores of the Zeeman-analyzed profiles are emphasized, during the reduction of photographic Zeeman-analyzed plates, the value of the longitudinal field inferred will deviate from its true value. Two values of the longitudinal field are obtained from the line profiles (H_{e3} and H_{e7}). They are derived from the theoretical Zeeman-analyzed line profiles when only the deepest 30 percent (H_{e3}) or 70 percent (H_{e7}) of the profiles (after convolution with an instrumental profile and application of a characteristic curve) are used in obtaining the separation of the Zeeman-analyzed components and therefore the longitudinal field. In Paper II it is shown that H_{e3} and H_{e7} are successful in reproducing the broad and narrow extrema, observed in several Ap stars, while the true values of the longitudinal field show nearly symmetrical curves. In Paper I it is shown that H_{e3} and H_{e7} , for very decentered dipole geometries, may not show the reversal of polarity expressed by the true longitudinal field. Figure 4 of Paper I shows the H_{e3} and H_{e7} curves for the same model chosen to approximate HD 10783. In figure 4 (this paper), the H_{e3} and H_{e7} curves have been plotted, after changing the sign and the theoretical phase convention with the observed longitudinal fields in Preston and Stepień (1968). The signs of H_{e3} and H_{e7} have been changed from the original paper: the strong pole is now taken to be negative. This sign change does not affect the radial velocity curve, as it depends on the field strength but not on its sign. We see that the H_{e3} and H_{e7} curves show a reasonable approximation to the magnetic curve of HD 10783 (a better fit can be attained with small changes in the input parameters) provided phase 0.0 of the models (strong surface field) is identified with

phase 0.5 of the magnetic curve of HD 10783. This provides a justification, valid in the framework of Papers I and II, for the fit between theoretical model and observations. It is apparent that HD 10783 is a good candidate for the effect proposed in the present work.

The effect should also be present in other Ap stars, acting in conjunction with radial velocity variations caused by nonuniform distribution of equivalent widths over the surface of the star. Thus, it should introduce errors in the harmonic analysis of Ap stars (Deutsch 1970) where only the nonuniform distribution of equivalent widths is assumed to cause variations. An interesting application of the mechanism proposed might be to detect evidence of magnetic fields in conditions in which other methods fail and to draw conclusions on the field geometry. For example, if the geometry of the magnetic field is such that a weak longitudinal field results from a fairly large surface field, the longitudinal field might be too small to be detected, but the spectral variations could betray its presence as they depend on the total field strength rather than on the longitudinal component alone. The detection of profile changes in stars rotating too rapidly to be observable with the usual photographic technique (Babcock 1962) could also be taken as evidence of magnetic field. The difficulty will reside in proving that the changes are caused by the Zeeman effect and not abundance variations or other atmosphere effects. The question could be resolved by observing strong saturated lines for which the effect of changing abundances should be minimal, or lines from ions which do not show conspicuous changes in equivalent width through the cycle. The dependence on the z -value is also a clue.

As an example of the usefulness of the effect proposed as applied to the understanding of the Ap stars, let us assume that it has been proved that the radial velocity variations in HD 10783 are caused by the Zeeman effect. From the radial velocity curve we can identify phase 0.5 as the part of the cycle for which the surface field is at maximum, the light curve is then at minimum. HD 10783 therefore would not appear to follow several other Ap stars which show maximum surface field at maximum light (Wolff and Wolff 1970).

III. SPURIOUS EQUIVALENT-WIDTH VARIATIONS

Figure 5 shows line profiles obtained from a model of Paper I at three points of the cycle. The rotation axis is perpendicular to the line of sight and to the dipolar axis. The decentering parameter is $a = 0.5$, the polar field is 30,000 gauss, and the equatorial velocity is taken to be negligible. We can see that the profile at phase 0.0 is different from the other two as it is shallower and has extended weak wings. The extended wings are formed by the widely separated σ components developed in the regions of large field, while the regions of a weaker field and all of the π

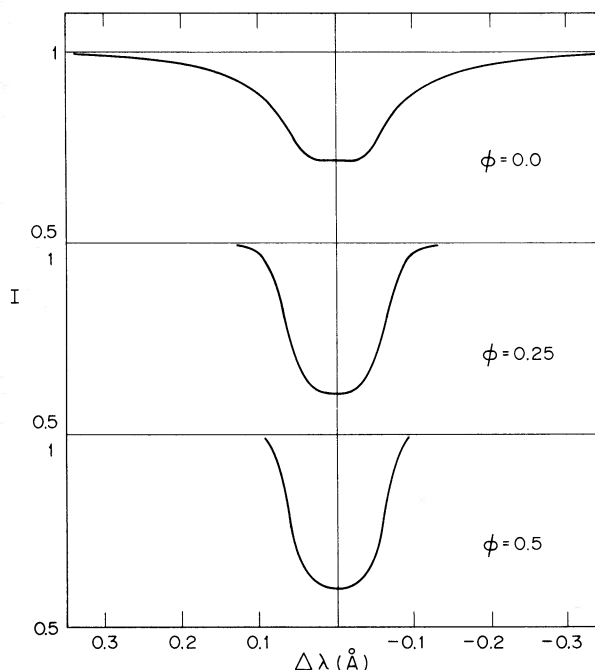


FIG. 5.—Line profiles at three points of the cycle for the model with negligible equatorial velocity. The graphs are identified by the phase ϕ .

components contribute to the core. At phase 0.0 the observer views the strong polar field (30,000 gauss) at the center of the disk and regions with fields less than a tenth of the polar field near the limb. At phase 0.5 the observer views the opposite hemisphere of the star, which has a weak, more uniform field. Thus we have a narrow line.

The extended wings at phase 0.0 would probably not be seen on a photographic plate, because of their weakness and because of blending with neighboring lines. Thus, not seeing the wings, one would have the impression of a change in equivalent width. The effect is not negligible if we consider that for a line above the shoulder of the curve of growth, a large change in abundance is needed to give a small change in equivalent width. We can expect apparent equivalent-width changes in any geometry where a large field occupying a relatively small portion of the star (such as a giant starspot) coexists with weaker fields. The large field region will have its σ components shifted out of the line, where they are not seen. This effect will be especially important for objects with small rotational velocities.

I wish to thank the Carnegie Institution of Washington for the award of a Carnegie Postdoctoral Fellowship, Dr. R. F. Howard for the use of the computing facilities of the Solar Division, and Dr. G. W. Preston for drawing HD 10783 to my attention and for useful discussions.

REFERENCES

- Babcock, H. W. 1949, *Ap. J.*, **110**, 126.
———. 1962, in *Astronomical Techniques*, ed. W. A. Hiltner
(Chicago: University of Chicago Press), p. 107.
Borra, E. F. 1974a, *Ap. J.*, **187**, 271 (Paper I).
———. 1974b, *ibid.*, **188**, 287 (Paper II).
Deutsch, A. J. 1970, *Ap. J.*, **159**, 985.
Landstreet, J. D. 1970, *Ap. J.*, **159**, 1001.
Preston, G. W. 1971, *Pub. A.S.P.*, **83**, 571.
Preston, G. W., and Stepień, K. 1968, *Ap. J.*, **154**, 971.
Unno, W. 1956, *Pub. Astr. Soc. Japan*, **8**, 108.
Wolff, S. C., and Wolff, R. J. 1970, *Ap. J.*, **160**, 1049.

ERMANNO F. BORRA: Hale Observatories, 813 Santa Barbara Street, Pasadena, CA 91101